Evaporation-induced monolayer compression improves droplet interface bilayer formation using unsaturated lipids

Guru A. Venkatesan, Graham J. Taylor, Colin M. Basham, Nathan G. Brady, C. Patrick Collier, and Stephen A. Sarles

Citation: Biomicrofluidics **12**, 024101 (2018); doi: 10.1063/1.5016523
View online: https://doi.org/10.1063/1.5016523
View Table of Contents: http://aip.scitation.org/toc/bmf/12/2
Published by the American Institute of Physics

Evaporation-induced monolayer compression improves droplet interface bilayer formation using unsaturated lipids

Guru A. Venkatesan,[1] Graham J. Taylor,[1,2,3] Colin M. Basham,[1] Nathan G. Brady,[4] C. Patrick Collier,[1,3,5] and Stephen A. Sarles[1]
[1]*Department of Mechanical, Aerospace, and Biomedical Engineering, University of Tennessee, Knoxville, Tennessee 37996, USA*
[2]*Bredesen Center, University of Tennessee, Knoxville, Tennessee 37996, USA*
[3]*Joint Institute for Biological Sciences, Oak Ridge National Laboratory, Oak Ridge, Tennessee 37831, USA*
[4]*Department of Biochemistry, Cellular and Molecular Biology, University of Tennessee, Knoxville, Tennessee 37996, USA*
[5]*Center for Nanophase Materials Sciences, Oak Ridge National Laboratory, Oak Ridge, Tennessee 37831, USA*

(Received 20 November 2017; accepted 13 February 2018; published online 1 March 2018)

In this article, we report on a new experimental methodology to enable reliable formation of droplet interface bilayer (DIB) model membranes with two types of unsaturated lipids that have proven difficult for creating stable DIBs. Through the implementation of a simple evaporation technique to condition the spontaneously assembled lipid monolayer around each droplet, we increased the success rates of DIB formation for two distinct unsaturated lipids, namely 1,2-dioleoyl-*sn*-glycero-3-phosphocholine (DOPC) and 1-palmitoyl-2-oleoyl-*sn*-glycero-3-phosphocholine (POPC), from less than 10% to near 100%. Separately, using a pendant drop tensiometer, we learned that: (a) DOPC and POPC monolayers do not spontaneously assemble into their tightest possible configurations at an oil-water interface, and (b) reducing the surface area of a water droplet coated with a partially packed monolayer leads to a more tightly packed monolayer with an interfacial tension lower than that achieved by spontaneous assembly alone. We also estimated from Langmuir compression isotherms obtained for both lipids that the brief droplet evaporation procedure prior to DIB formation resulted in a 6%–16% reduction in area per lipid for DOPC and POPC, respectively. Finally, the increased success rates of formation for DOPC and POPC DIBs enabled quantitative characterization of unsaturated lipid membrane properties including electrical resistance, rupture potential, and specific capacitance. *Published by AIP Publishing*. https://doi.org/10.1063/1.5016523

INTRODUCTION

The structure and composition of cellular membranes play essential roles in maintaining healthy cell and organelle functions, which is why cells actively regulate which lipid types are present in their various membranes.[1] Changing the lipid composition of a cell membrane can affect many physical properties, including thickness, bending modulus, intramembrane potential, and permeability of the bilayer, to name just a few. Variations in the lipid composition also directly affect the interaction with and function of transmembrane proteins.[2,3] These dependencies thus motivate careful consideration of lipid choice for the assembly and study of simplified model membranes, including liposomes and planar lipid bilayers.

The droplet interface bilayer (DIB) approach for creating planar model membranes yields a planar lipid bilayer at the interface between adjoined lipid-coated water droplets in oil.[4,5] The DIB method has gained interest in recent years because of key experimental advantages, including: a relatively simple experimental setup (i.e., no nano-porous substrate is required) and methodology (i.e., bringing droplets into contact does not require significant skill), the ability to control lipid composition for each leaflet of the membrane, and access to both sides of the bilayer

for quantitative electrophysiological measurements.[6–8] These advantages have enabled researchers to utilize DIBs to study various properties of membranes such as water permeability,[7] lipid phase behavior,[9,10] and lateral diffusion of lipids and proteins,[11] and to develop various types of bio-inspired and bio-derived sensors using lipids (both synthetic and natural extracts[10,12]), proteins, and synthetic polymers.[12–14]

The formation of a stable DIB hinges on spontaneous self-assembly of lipids to form a "well-packed" monolayer at the oil-water interface around each droplet. Failure to achieve sufficiently packed lipid monolayers leads to coalescence upon droplet contact, rather than bilayer formation.[15,16] Results from the few published attempts to characterize the conditions required to successfully assemble a DIB suggest that, in addition to using a sufficiently *thermodynamically poor* (i.e., energetically less favorable) organic solvent for the acyl chains,[17] a "well-packed" monolayer with an interfacial tension (IFT) of 1–2 mN/m is necessary.[16,18]

While achieving low IFT is proven to be a prerequisite, anecdotal evidence obtained in our own work suggest that monolayers formed by certain lipids, even those with IFT values of ~1–2 mN/m in suitable solvents, fail to form a stable DIB. For instance, it is well known from literature that 1,2-diphytanoyl-*sn*-glycero-3-phosphocholine (DPhPC) phospholipids quickly self-assemble (<5 min) at a water-alkane (e.g., decane, hexadecane) interface to form "well-packed" monolayers with IFTs of ~1.2 mN/m and yield a near 100% DIB formation success rate in the same oils.[16] However, 1,2-dioleoyl-*sn*-glycero-3-phosphocholine (DOPC) lipids, which also self-assemble in only a few minutes to form monolayers with similar values of IFT (<2 mN/m), rarely form stable DIBs (5%–10% success rates) after the same amount of time for incubation in oil.[16]

Owing to its high repeatability and subsequent bilayer stability, DPhPC—a saturated lipid native to archaeal organisms—has been the most common lipid of choice for DIB formation to-date.[12] In contrast, DOPC—an unsaturated phospholipid containing oleic acyl chains common to eukaryotes and often used to model mammalian cell membrane compositions[1]—is used less often in DIB formation. Interestingly, nearly all studies on DOPC DIBs have utilized microfluidic environments and droplet volumes less than 100 nl to achieve consistent DIB formation (see Table S1 in the supplementary material). In a recent exception,[19] Barlow *et al.* reported stable DIB formation between large, 900 nl DOPC-coated droplets, though only after more than 40 min of incubation in oil.

To improve DIB formation with DOPC, other groups have recently shown that amphiphilic compounds (such as SDS and SPAN) used as co-surfactants with lipids promote sufficient monolayer formation and enable the assembly of stable DOPC DIBs even with large droplets.[20–22] These findings were explained in the context of lipid-shape factor; addition of co-surfactants with a conical shape that compliments the inverted conical shape of DOPC enables tighter monolayer packing and a better coverage of the oil-water interface. However, the presence of surface active polymers in a lipid-based monolayer or bilayer is known to alter the transport properties of the membrane and, more importantly, may not accurately mimic the membranes of living cells.[23,24] Thus, there remains a need for understanding why unsaturated phospholipids like DOPC fail in DIB formation despite their low equilibrium surface tensions, as well as new experimental methods to improve DIB formation from biologically relevant unsaturated lipids such as DOPC and with droplets that can be easily dispensed with a standard micropipette (>100 nl)—a key in the simplicity of the DIB method.[25]

Here, we report on a quick and simple droplet evaporation technique that provides lateral compression to the spontaneously assembled monolayers around the droplets to improve DIB formation with unsaturated phospholipids. We show that this approach achieved stable DIBs with near 100% success. The two unsaturated lipids chosen for this study included DOPC and POPC (1-palmitoyl-2-oleoyl-*sn*-glycero-3-phosphocholine); both are in the liquid-disordered phase at room temperature and are commonly used to model eukaryote cell membranes. Importantly, application of this evaporation technique obviates the usage of polymer-based co-surfactants in a biomimetic system that is highly sensitive to composition, instead yielding stable, phospholipid-only DIBs. To understand how this technique improved bilayer formation, we quantified the effects of evaporation-induced lateral compression on unsaturated lipid

monolayers using pendant drop tensiometry and Langmuir isotherms and made comparisons to identical measurements of DPhPC monolayers. Lastly, we measured membrane electrical resistance, specific capacitance, and rupture potential with stable DOPC, POPC, and DPhPC DIBs to show that these unsaturated model membranes are suitable for a variety of electrophysiology studies.

METHODS

DIB formation

Lipid-in DIBs were formed on the ends of wire-type electrodes as described in the supplementary material. A minimum of 5 DIB assembly trials were performed for each lipid-oil combination to assess the effect of intentional droplet evaporation on the bilayer formation success rate. Stable bilayers were electrically characterized following previously reported techniques[26,27] to obtain the resistance, rupture potential, and specific capacitance (C_M).

Pendant drop tensiometry

Interfacial tension (IFT) measurements were used to quantitatively characterize the self-assembly of lipid monolayers at an oil-water interface. Two types of IFT measurements—fixed-volume IFT followed by volume reduction IFT step-response—were performed in sequence using pendant drop tensiometry (PDT). In fixed-volume IFT measurements, equilibrium IFT values of unperturbed (i.e., spontaneously assembled) monolayers were measured following an established procedure reported elsewhere.[16] Next, the automated volume control device of the tensiometer was used to reduce the volume of pendant drop in small ($\sim$0.08 to 0.50 μl) steps while continuously measuring the IFT. These volume reductions were performed to emulate the evaporation-induced volume shrinkage performed in DIB experiments.

Monolayer compression isotherm

Monolayer compression isotherms were measured for each lipid type to quantify the area occupied by each lipid molecule and identify the differences in their compressibility properties. Five trials were recorded for each lipid type using steps described in the supplementary material and the averages of surface pressure (Π) and area (A) were plotted.

RESULTS

Improved DIB formation with evaporation-induced monolayer compression

In a conventional lipid-in DIB experiment, droplets containing liposomes at a concentration of 1–10 mg/ml are incubated in oil at a temperature above the phase transition temperature of the lipid(s)[10,12] for several minutes to promote monolayer formation prior to bringing the droplets into contact [Fig. 1(a)]. However, we and others[21,22] have observed that some types of lipids, including unsaturated lipids such as DOPC and POPC, fail to form well-packed monolayers capable of yielding a stable bilayer—i.e., droplets placed in contact coalesce [Fig. 1(b)] rather than form an interfacial bilayer.

Herein, a controlled droplet evaporation procedure was performed prior to bringing droplets into contact under oil. The premise for improving the success rate of DIB formation is that a loss of volume of an aqueous droplet pre-coated with a partially packed monolayer reduces the surface area of the droplet, which will result in lateral compression and tighter packing of the adsorbed phospholipids. In turn, this increased packing should aid or enable bilayer formation upon droplet contact. Thus, while Sandison *et al.* used evaporation of the organic solvent to accelerate thinning of substrate supported black lipid membranes (BLMs),[28] our approach harnesses evaporation to condense the monolayer on each droplet, prior to the process of bilayer formation.

The sequence of our technique is illustrated in panels (a), (c), and (d) in Fig. 1. Specifically, after incubating droplets in oil for 5 min to facilitate the formation of droplet surfaces partially packed with lipids [Fig. 1(a)], droplets were brought close to the oil-air interface

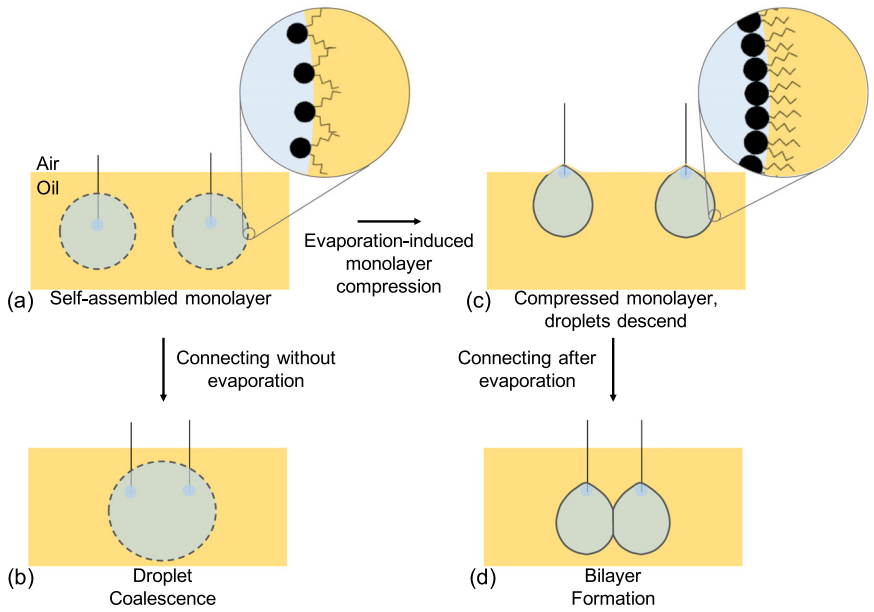

FIG. 1. Schematics showing unsaturated lipids leading to droplet coalescence (a → b) and application of evaporation-induced monolayer compression leading to successful DIB formation (a → c → d).

and held for 10–60 s. Because it was difficult to assess distances between the contoured oil-air surface and the top of the droplet, positioning was performed in such a way that the ball-end electrodes holding the droplets were pressed vertically against the oil-air interface [Fig. 1(c)], where a thin ($\lesssim$100 μm) layer of oil was retained between the top of the water droplet and the oil-air interface. Droplets shrank rapidly at this location due to a higher water evaporation rate (1409 ± 270 $\mu m^2/s$) compared to droplets fully submerged in the oil ($\sim$8.33 $\mu m^2/s$).[29] This intentional shrinkage incurred visual changes to the droplets. Before droplet evaporation, water droplets with poorly coated monolayers were observed to be positioned on electrodes in such a way that the agarose-coated electrode tip and the waist of the droplet were in the same horizontal plane [Fig. 1(a)]. This indicated a relatively high interfacial tension that correlated to a partially packed monolayer, and the resulting droplets were fairly spherical and drawn upwards on the electrode. Upon shrinkage at the oil-air interface, we observed the waist of each droplet to fall below the agarose-coated electrode tip; the droplets "slid" down the electrodes and also sagged vertically into a non-spherical shape, as shown in Figs. 1(c) and 1(d). This change in the droplet position on the horizontal plane was used qualitatively as a visual cue for the interfacial tension reaching a minimum point that signaled the completion of monolayer formation and packing. The electrodes were then lowered away from the air-oil interface, into the bulk oil, to halt additional evaporation and the droplets were brought into contact to initiate DIB formation. Figure 2 shows images of DOPC-coated droplets hanging from electrodes in oil

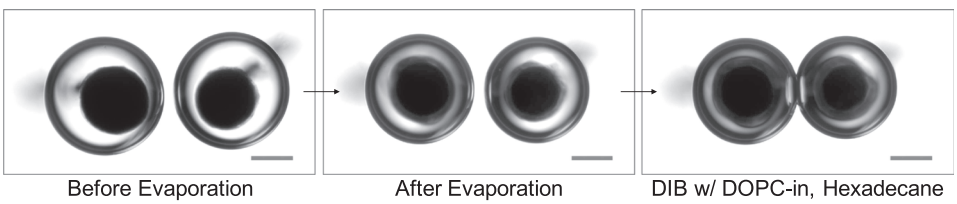

FIG. 2. Micrographs of 300 nl aqueous droplets containing DOPC liposomes placed under hexadecane before and after evaporation at the oil-air interface. The micrograph on the right shows the successful formation of a stable DIB after implementing the evaporation step. Scale bar: 300 μm. In this representative trial, the apparent waist radii of the left and right droplets were reduced by 7% and 10%, respectively.

collected: before evaporation, after evaporation, and after the formation of a stable droplet interface bilayer. In some cases, we observed droplets to completely fall off the electrodes due to the very low IFT obtained during the evaporation step. Nonetheless, DIB formation could still be assessed: electrodes were gently re-inserted into the droplets using micromanipulators and the droplets were placed into contact.

The experimental result was concluded to be successful if a DIB formed upon contact between droplets and was found to be stable, without droplet coalescence, for at least 1 min. Bilayer formation was determined both by visual confirmation of droplet adhesion (see right panel in Fig. 2) and via electrical measurement of the increase in capacitance resulting from exclusion of oil from the thinning interface. The experiment was noted to fail if the droplets coalesced either immediately upon contact or during bilayer thinning and radial expansion. As summarized in Table I, we observed that implementing the evaporation step drastically improved DIB formation success rates for both unsaturated lipid types in two different alkanes: hexadecane (C16) and dodecane (C12). Across both types of oils and lipids, a 90%–100% DIB formation success rate was recorded when droplets were connected following brief evaporation. Once successfully formed, DOPC and POPC DIBs were found to remain intact for longer periods of time (e.g., 30–40 min at the minimum, which is the duration of a typical electrical characterization test). The values for membrane resistance and rupture potential provided in Table I further testify to the stabilities of the DIBs formed using DOPC and POPC. Because DPhPC is well known to spontaneously assemble into a tightly packed monolayer,[16] we observed no need for evaporation to achieve stable DIBs in either alkane. However, we found that performing the evaporation step did not reduce the ability to achieve a stable DIB with DPhPC (Table I). A specific capacitance of c.a. 0.63–0.69 μF/cm^2 for all three lipid types suggested similar hydrophobic thicknesses in hexadecane,[27] however POPC bilayers in dodecane exhibited a far smaller decrease in specific capacitance to c.a. 0.55 μF/cm^2 in dodecane as compared to DPhPC (c.a. 0.39 μF/cm^2) and DOPC (c.a. 0.36 μF/cm^2). This finding suggested the saturated palmitoyl acyl chain of the POPC lipid favors greater exclusion of dodecane upon bilayer formation compared to both the double unsaturated acyl chains of DOPC and the bulky and methylated saturated chains of DPhPC.

DYNAMIC INTERFACIAL TENSION MEASUREMENTS

The spontaneous assembly of a lipid monolayer at the surface of a water droplet in oil results in a measurable reduction in IFT. Therefore, we also performed IFT measurements to quantitatively compare dynamic spontaneous monolayer assembly for unsaturated lipids

TABLE I. Number of successful DIB formation trials with and without the evaporation step and the electrical measurements obtained from the successful trials.

DIB formation success rate

Alkane	Condition	DPhPC	DOPC	POPC
Hexadecane	Without evaporation	10/10	2/20	0/10
	With evaporation	10/10	9/10	9/10
Dodecane	Without evaporation	5/5	2/6	0/6
	With evaporation	3/3	7/7	9/12

Electrical properties of DIBs

	Resistance (MΩ cm^2)		Max. rupture potential (mV)		Specific capacitance (μF cm^{-2})	
Lipid	Hexadecane	Dodecane	Hexadecane	Dodecane	Hexadecane	Dodecane
DPhPC	8.04 ± 3.6	6.47 ± 1.1	275	200	0.685 ± 0.07	0.386 ± 0.07
DOPC	1.99 ± 0.88	2.78 ± 0.71	150	100	0.652 ± 0.08	0.357 ± 0.07
POPC	1.03 ± 0.68	3.53 ± 2.2	100	125	0.626 ± 0.05	0.553 ± 0.13

compared to DPhPC and, separately, to estimate the additional reduction in IFT incurred by evaporation as applied to improve DIB formation success rates. First, IFT measurements performed using fixed-volume (1 μl) PDT revealed that DPhPC and DOPC lipids, when placed as liposomes in aqueous droplets (i.e., lipid-in Ref. 6), self-assembled at a hexadecane-water interface to form monolayers with equilibrium IFT (γ) values of 1.18 ± 0.2 mN/m and 1.99 ± 0.5 mN/m, respectively, within 5 min [Fig. 3(a)]. The surface pressures ($\Pi = 44$ - γ; >42 mN/m) of both these monolayers were above the bilayer-monolayer equivalence pressure of 40 mN/m,[30] and, thus, were both expected to be suitable for DIB formation. While Table I shows that this surface pressure correlated to sufficiently packed monolayers for bilayer formation in the case of DPhPC-coated droplets, we recorded an 80% failure rate in attempts to assemble DIBs from DOPC monolayers after 5 min of monolayer assembly in hexadecane (Table I). In the case of POPC, the IFT did not reach a stable value even after 15 min of spontaneous self-assembly (a quasi-equilibrium value of 12.68 ± 1.9 mN/m is recorded after 15 min), indicating the formation of a sparsely packed monolayer. This finding explains why POPC-coated droplets that were not intentionally evaporated coalesce (100% failure rate) instead of forming a stable DIB (Table I). The fact that intentional droplet evaporation improved DIB formation for both DOPC and POPC indicates that it is possible, and perhaps required, to further reduce the IFT of a partially packed monolayer to a point at which DIB formation is possible.

Next, we performed successive, step-wise reductions in pendant droplet volume while continuously measuring IFT to investigate how droplet shrinkage at the air-oil interface in DIB experiments affected the IFT of a pre-assembled monolayer [see Fig. 3(b)]. Note that in this technique, while the volume of the pendant droplet exposed to the oil decreased, the concentration of lipids remained constant. Figures 3(c)–3(e) shows sample IFT responses for volume reduction steps performed on monolayers after reaching an equilibrium IFT (~5 min for DPhPC and DOPC) or after 15 min of incubation of droplets in oil for POPC. Because POPC-coated droplets exhibited the smallest spontaneous reduction in IFT, each volume reduction step performed on a POPC monolayer further reduced the IFT, likely by the lateral compression of pre-adsorbed lipids at the interface. Eventually, a minimum IFT value of less than 1 mN/m was consistently observed as shown in Fig. 4(a) (i.e., $\gamma_{15min} \gg \gamma_{saturation}$), which shows how IFT

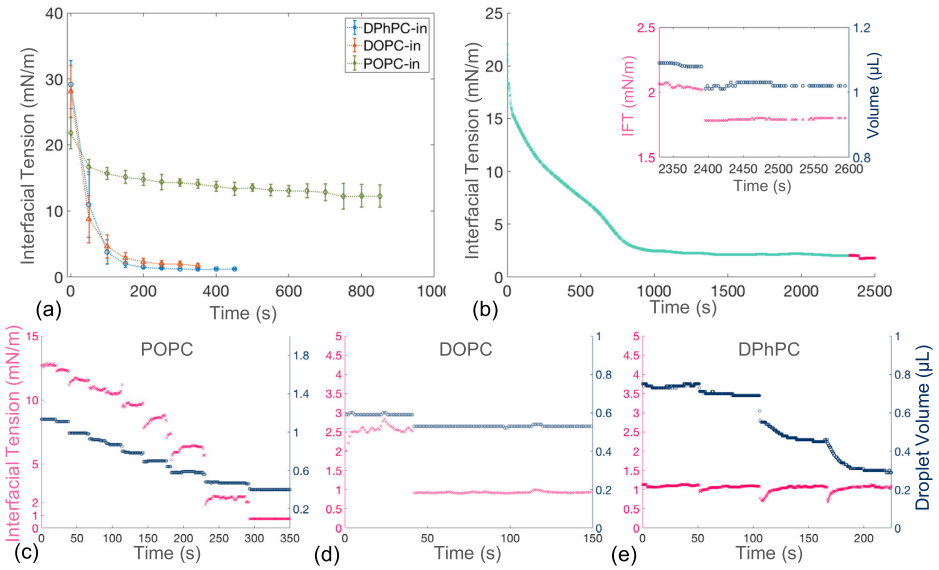

FIG. 3. (a) Temporal change in interfacial tension of a hexadecane-water interface for DPhPC (blue, □), DOPC (red, Δ), and POPC (green, O) as measured by the pendant drop tensiometer. Each IFT data marker represents the average of 3 or more measurements that are performed in the constant volume mode. (b) Change in interfacial tension measurement during spontaneous monolayer formation (green) and during step-wise volume reduction (pink) after reaching equilibrium IFT. Inset: closer look at the change in IFT due to a single volume reduction step. Representative IFT traces showing change in tension (pink) induced by step-wise reduction in the droplet volume (blue) for POPC (c), DOPC (d), and DPhPC (e).

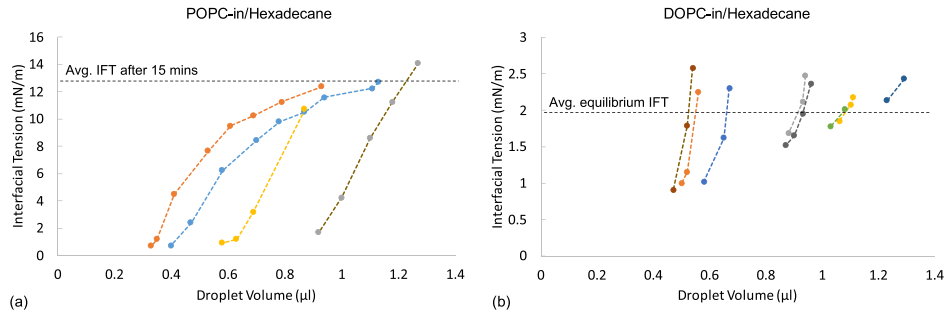

FIG. 4. Change in IFT induced by step-wise volume change for multiple trials of POPC (a) and DOPC (b) monolayers. Initial lipid concentration in aqueous droplets was 2 mg/ml. The dotted lines in these plots are a guide to the eye. Different trajectories seen in (b) are due to different time intervals between each step.

decreased with shrinking droplet volume for multiple measurements on DOPC and POPC-coated pendant droplets. In the case of DOPC [Fig. 4(b)], the volume reduction step was performed once the IFT reached a value within 1 mN/m of the average value of IFT at equilibrium recorded using fixed-volume PDT. We observed the volume reduction steps to result in a stable value of IFT below 1 mN/m, suggesting even tighter lateral packing of lipids than achieved by spontaneous assembly alone (i.e., $\gamma_{spontaneous} > \gamma_{saturation}$). A similar effect of reduction in DOPC monolayer IFT (from equilibrium 4.8 to 1.2 mN/m) was reported upon adsorption of a globular protein, lysozyme.[31] In the case of DPhPC, however, volume reduction steps performed after reaching equilibrium did not result in a stable reduction of IFT. Instead, the measured tension rebounded to its equilibrium value after a transient response to the volume reduction [Fig. 3(e)]. This finding suggests that the spontaneously assembled DPhPC monolayer was already in its tightest packing configuration (i.e., $\gamma_{spontaneous} \approx \gamma_{saturation}$). As a result, evaporation did not yield a sustained increase in the lateral packing of lipids; i.e., exclusion of excess lipid molecules from the compressed monolayer through buckling forced a rebound in transient IFT.[32,33] This incompressibility was further supported by the higher stiffness values exhibited by compressed DPhPC monolayers at high surface pressures as shown in Fig. S1(b), supplementary material.

The data shown in Fig. 4 provide strong evidence that spontaneously assembled DOPC and POPC monolayers can be compressed further by reducing drop volume, and thus drop surface area available to the monolayer lipids, to achieve tighter lipid packing and lower values of IFT than was achieved through spontaneous assembly alone. The resulting increase in lipid packing is in direct agreement with our findings (Table I) that controlled droplet evaporation greatly enhances DIB success for DOPC and POPC.

COMPRESSION ISOTHERM MEASUREMENTS

The observed decreases in IFT caused by reductions in droplet volume motivate the need for further characterizing changes in lipid packing. Compression isotherms of pure DPhPC, DOPC, and POPC monolayers at an air-water interface are shown in Fig. S1 (supplementary material), and each isotherm shows a smooth response with surface pressure continuously increasing as lipids were compressed. Surface pressure reaches a maximum and plateaus, a phenomenon associated with buckling of the monolayer lipids compressed to their maximum allowable extent, for all lipid cases.[33] The surface pressure-area isotherms contain no sharp transitions like those expected in the case of a compression-induced transition from the liquid expanded to the liquid condensed phase, proving that all three types of monolayers remained in the liquid expanded phase during compression to the point of buckling. These measured isotherms and collapse pressure values (Table S2, supplementary material) are in good agreement with previous reports,[21,34–36] and they highlight differences in the average area occupied per lipid at a given surface pressure. Specifically, a single DPhPC molecule takes up a larger area

(63.9 Å^2) compared to both DOPC (53.6 Å^2) and POPC (50.3 Å^2) at their respective collapse pressures (i.e., maximum pressure before monolayer buckling).

DISCUSSION

Self-assembled lipid monolayers are essential for creating droplet interface bilayers,[4] and it is well established that both the kinetics and equilibrium packing density of monolayer formation at an oil-water interface are directly influenced by the concentration of the lipids. Generally, the number of amphiphiles at the interface increases as the lipid concentration increases in the bulk. However, Needham *et al.*[37] demonstrated that increasing the lipid concentration in the bulk beyond the critical micelle concentration (CMC) does not yield further increases in surface density (i.e., decreases in interfacial tension). In this work, we studied monolayer formation with three types of lipids introduced into the aqueous phase at an initial concentration of 2 mg/ml, which is well above the CMCs (∼0.1–10 μM) for all three lipids (CMC measurements are described in the supplementary material and data are presented in Figs. S2 and S3, and Table S3). A starting concentration above CMC implies that lipid assembly in these experiments was not diffusion limited, and it also suggests that a higher lipid concentration, achieved either by a higher initial concentration in the droplet or incurred passively upon evaporation of water, is insufficient to achieve a higher equilibrium packing density in the monolayer. As a simple test of this theory, we also attempted DIB formation between POPC-coated droplets containing 10 mg/ml of lipids and observed similar difficulty (without evaporation) and success (with evaporation) as reported in Table I for 2 mg/ml.

To create a DIB, two or more aqueous droplets each coated with a well-packed lipid monolayer are connected under a suitable organic solvent. If the droplet interfaces are bare or sparsely coated with lipids, the interfacial tension between the oil-water interface remains high (as high as 44 mN/m). When two or more such droplets are brought into contact, the high tension creates a thermodynamic drive to fuse the droplets to minimize the total surface energy of the system, since the surface area of a fused droplet is considerably lower than the total surface area of two separate droplets. In contrast, the presence of sufficiently packed lipid monolayers around both droplets enables the system to reduce its free energy by the amount $\Delta F = A \times (2\gamma_m - \gamma_b)$ through the formation of an oil-depleted interface bilayer, where A is the area of the bilayer, γ_m is the tension of the monolayer, and γ_b is the bilayer tension.[38] The stable adhesive state of the droplets represents a local energy minimum with a total energy greater than that of coalesced droplets.[17] While several lipid types are known to readily self-assemble to form well-packed monolayers at room temperature, there is also substantial evidence in the literature that monolayers formed by certain lipids are more suitable than others for DIB formation.[12] Specifically, unsaturated lipids such as DOPC and POPC often fail to form DIBs between droplets larger than 100 nl in volume. In contrast, several groups have reported the assembly and study of stable DOPC DIBs when droplet volumes are <100 nl (Table S1, supplementary material).

The IFT measurements provided in Figs. 3 and 4 provide insights into the effectiveness of monolayer formation for the three lipids studied herein and help to explain the DIB formation success rates presented in Table I. DPhPC lipids spontaneously assembled to form a tightly packed monolayer with an IFT that could not be further reduced via reduction in the droplet surface area. This result confirmed our ability to form DPhPC DIBs without performing droplet evaporation. On the other hand, POPC lipids self-assembled to form a sparsely packed monolayer that was further compressed by reducing the volume (and area) of the aqueous droplet. Our measurements using PDT demonstrated that aqueous volume reductions stably reduced the IFT of the monolayer-coated interface to below 1 mN/m. Lastly, while DOPC lipids spontaneously assembled to form monolayers with an average equilibrium IFT of ∼2 mN/m—a value that we expected to be sufficient for DIB formation—we found that these monolayers can also be further compressed to reach a minimum IFT of <1 mN/m. These findings showing compression-induced reduction in IFT with both POPC and DOPC correlate well to our observations that evaporation improved DIB formation in both hexadecane and dodecane. Given

these outcomes, it was necessary to understand what about the structure of a lipid prevents spontaneous assembly of a densely packed monolayer, as well as how much lateral compression of the monolayer occurred when droplets were prescribed this new droplet shrinking protocol.

Differences in equilibrium packing densities (and IFT values) between the three lipids studied can possibly be explained by structural differences brought about by the lipid shape and the extent to which alkane molecules from the surrounding oil partition in between the tail groups. All three lipids under consideration are made up of identical phosphatidylcholine (PC) head groups. However, their tail groups vary in length and composition. DPhPC has two fully saturated 16C fatty acid chains with 4 methyl groups attached to each chain, whereas DOPC is made up of two 18C fatty acid chains with a single double-bond (Δ9-Cis) in each chain. Lastly, POPC is a hybrid-monounsaturated lipid that is made up of one fully saturated 16C chain and one mono-unsaturated 18C (Δ9-Cis) fatty acid chain. These double bonds found in the tail groups of DOPC and POPC are known to induce a bend (often referred to as "kink") in the tail—a restricted rotation about the double-bound that is not found in fully saturated tail groups of DPhPC. These kink(s) give both DOPC and POPC molecules conical shapes (DOPC being more conical than POPC[3]). Our data suggests the conical shapes of DOPC and POPC prevent efficient lateral packing and favor the persistence of defects in monolayers and bilayers. DPhPC molecules, on the other hand, take on a more cylindrical shape that allows them to efficiently pack to form defect-free planar monolayers and bilayer membranes.[3,39–42]

As lipids self-assemble to form a monolayer at an oil-water or air-water interface, the intrinsic shapes of the amphiphilic molecules dictate the extent to which the IFT is reduced. In the case of cylindrically shaped DPhPC, the lipid molecules spontaneously assembled to their tightest packing state at equilibrium, retaining minimal packing defects [Fig. 5(a)] and giving rise to low IFT. However, due to the steric hindrance posed by the conical-shape of neighboring unsaturated lipids, DOPC and POPC molecules failed to form a planar monolayer that is packed to its tightest packing state.[43] Instead, we believe self-assembled monolayers of these unsaturated lipids retained a significant degree of packing defects at equilibrium, which in turn led to an equilibrium IFT higher than the lowest possible IFT achievable by these monolayers.[31,44] While lipid shape describes why unsaturated lipids are unable to pack as tight as saturated DPhPC lipids at equilibrium, it does not explain why POPC lipids, despite being more cylindrical than DOPC,[3] self-assembled the slowest of the three lipids. In addition to lipid shape, other factors such as stability of liposomes and solubility of lipid tails in alkane may play roles in determining the rate of monolayer formation.

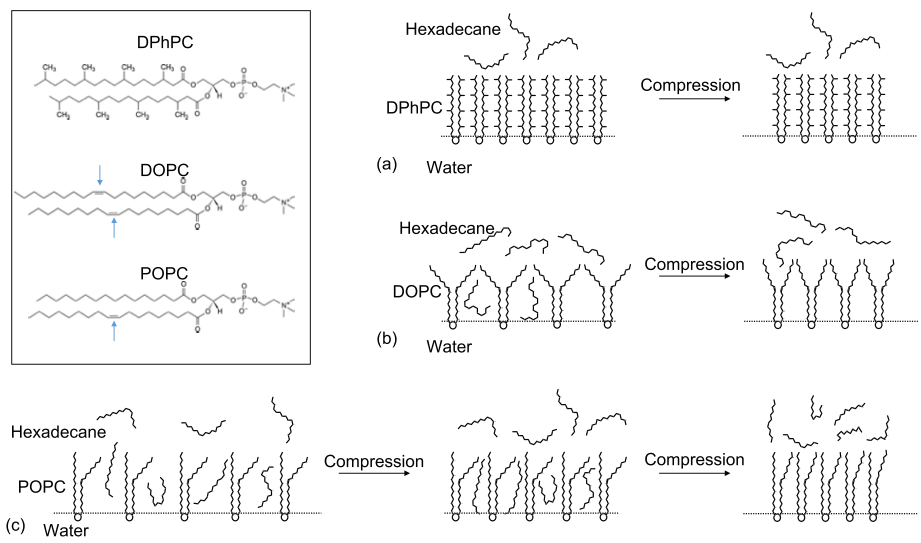

FIG. 5. Sketch showing organization of DPhPC (a), DOPC (b), and POPC (c) molecules and hexadecane molecules in a monolayer formed at a hexadecane-water interface before and after compression. The chemical structures of lipids are provided in the inset with arrows pointing at the double-bonds found in the fatty acid chains.

The excess area (i.e., packing defects) created by the kinks of unsaturated tail groups at a water-oil interface are expected to be occupied by alkane molecules found at the interface. Moreover, the presence of alkanes in the acyl chain regions of the monolayer may even provide an additional impediment to tight monolayer packing. X-ray diffraction studies have revealed that non-surface active molecules such as alkanes partition in between the hydrocarbon tail groups in a monolayer and change its packing and thermodynamic properties.[45–49] Compression isotherm experiments by Thoma and Möhwald revealed that higher amounts of alkanes partition among the lipid tail groups when the length of hydrocarbon chains is comparable to that of lipid tails.[50] Therefore, we suspect that self-assembled monolayers of DOPC and POPC possess packing defects that favor the partitioning of alkane molecules between the tail groups, as shown in Figs. 5(b) and 5(c). Therefore, reducing the area available for each lipid by laterally compressing the monolayer: (a) forces the lipids to pack closer to one another, and (b) squeezes out residual solvent molecules found in the defects.[50] The combination of these two processes reduces the IFT of the monolayer laden oil-water interface by lowering the water-acyl chain and water-solvent molecule interactions. As the initial lipid concentrations for all experiments were significantly higher than their respective CMC values, the increase in packing density due to evaporation is expected to be dominated by the decrease in surface area and not due to the increase in lipid concentration in bulk. While it is possible that lateral compression of a monolayer could also lead to *cis-trans* isomerization of unsaturated acyl chains as seen during monolayer phase change, results from our experiments are inadequate to evaluate this effect.[51]

Next, we attempted to quantify the extent to which evaporation-induced droplet shrinkage prior to DIB formation decreased the area occupied by each lipid molecule. Figure S1 (supplementary material) shows how decreasing the average area available for lipid molecules changes the surface pressure of the monolayer formed at an air-water interface for all three lipid types. Because a direct comparison of IFT measured at the oil-water interface (using PDT) and surface pressure measured at the air-water interface (using Langmuir compression isotherm) was not possible, we made our comparison by equating measured changes in pendant droplet interfacial tension ($\Delta\gamma$) upon droplet shrinkage with changes in surface pressure ($\Delta\Pi$) upon lateral monolayer compression. Assuming the minimum tension ($\gamma_{saturation}$) reached in PDT measurements (Fig. 4) corresponded to the collapse pressure (Π_c) in the compression isotherm (Fig. S1, supplementary material) for the given lipid type, we estimated the change in area per lipid induced by the volume reduction steps. The filled circles in Fig. 6(a) represent the collapse pressures, which were assumed to correspond to the average minimum γ in PDT measurements ($\sim$1 mN/m for both DOPC and POPC, Fig. 4). The total change in tension attained by volume reduction steps is given by $\Delta\gamma = \gamma_{spontaneous} - \gamma_{saturation}$. Subtracting ΔIFT from collapse pressure should give us the surface pressure that was achieved by spontaneous assembly alone, i.e., $\Pi_{\text{spontaneous}} = \Pi_c - \Delta\gamma$. These values of $\Pi_{spontaneous}$ for DOPC and POPC are marked by open circles in Fig. 6(a). Performing this calculation enabled us to: (a) estimate the area per lipid molecule in the monolayer that was attained by spontaneous assembly alone, and (b) calculate the change in the area per lipid molecule brought about by the step-wise volume reduction. According to this analysis, each DOPC molecule in a spontaneously assembled monolayer occupied about 50.6 Å^2, which is $\sim$3 Å^2 (6%) higher than the area at maximum packing (collapse pressure). In the case of POPC, each molecule in the monolayer attained at the end of 15 min of incubation occupied approximately 42.3 Å^2, which is $\sim$8 Å^2 (16%) more area than at its maximum packing.

The area compression analysis discussed above can also be used to estimate the extent of droplet volume shrinkage required to successfully form DIBs with DOPC and POPC. According to this analysis, to achieve the tightest packing configuration, a maximum of 16% (6% for DOPC and 16% for POPC) reduction in area per molecule was predicted to be sufficient to bring about the required packing for DIB formation. Assuming a lipid-coated aqueous droplet to have a spherical shape, a 300 nl droplet has a surface area of 2.17 mm^2. A 16% reduction in surface area leads to a droplet with a final surface area of 1.82 mm^2 (231 nl), which is nearly a 23% reduction in volume. Depending on the initial packing state of monolayer before evaporation, the level of humidity in the local environment, and proximity of water

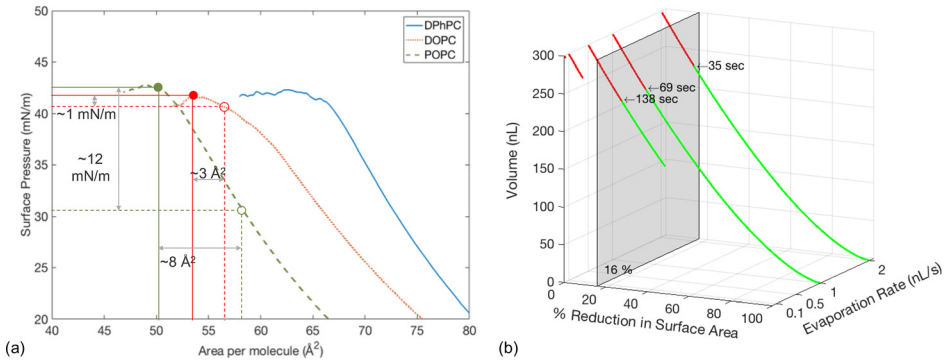

FIG. 6. (a) Area reduction analysis. Compression isotherms indicating collapse pressures (shaded circles) and estimated pressure and area per molecule corresponding to spontaneously assembled monolayer (unshaded circles). (b) Estimated percentage decrease in the droplet surface area caused by evaporation of a 300 nl spherical droplet at different rates of evaporation for 5 min. The reference plane shown in gray indicates the recommended 16% decrease in surface area required to achieve a tightly packed monolayer. Time value indicated next to each trend is the length of time required for the droplet surface area to reduce by 16%.

droplets to the oil-air interface during the evaporation step, a mere 10–60 s evaporation at the oil-air interface was found to be sufficient to achieve the packing required for successful DIB formation. Figure 6(b) shows the change in droplet volume and percentage reduction in the surface area of a spherical droplet with an initial volume of 300 nl that is subjected to evaporation at different rates of volume loss; see Fig. S4 (supplementary material) for percentage change in the surface area for different initial volumes. This simulation gives an insight to the period of time a droplet should be held at the oil-air interface in order to surpass the threshold percentage reduction in the surface area. Beyond this threshold (denoted by green line), the droplet is expected to retain a monolayer in which the lipids are packed in their tightest configuration and suitable for DIB formation. Excessive droplet shrinkage beyond the threshold is expected to lead to monolayer buckling, by which surplus lipids are excluded to maintain maximal packing in the monolayer.[32,33]

Finally, a few comments regarding the methodologies used herein. First, the IFT data measured using PDT were obtained with droplet volumes of only 1–2 μl. Because the accuracy of computing tension values can be compromised by small droplets that do not exhibit significant deformation, we computed the Worthington number,[52] W_o, given by $W_o = \Delta\rho g V_d/\pi\gamma_m D$ to verify the accuracy of the measurements. In this expression, $\Delta\rho$ represents the density difference droplet phase and the external oil phase, V_d is the volume of droplet, g is the acceleration due to gravity, γ_m is the monolayer IFT, and D represents the diameter of the dispensing needle. A value of W_o close to 1 indicates high precision in measuring IFT, while a value close to 0 indicates low precision. We estimated W_o to be between 0.6 and 0.9.

Second, the comparative analysis of IFT and compression isotherm data in Fig. 6(a) was only performed to obtain an estimate of possible area change obtained by lateral compression. The absolute values of the estimated change in area are subject to some variability based on the accuracy of either measurements. Primarily, values of molecular areas for lipids presented in the compression isotherms are sensitive to experimental procedures and are found to be highly variable in literature.[53] Third, the evaporation period estimated in Fig. 6(b) is likely overestimated, due to our assumption that droplets remain spherical. In reality, we know and observe that a droplet hanging from a slender electrode has a pendant-like shape [Fig. 1(c)], which causes it to undergo faster reductions in surface area compared to a spherical volume losing volume at the same rate. However, because it is difficult to accurately calculate the volume change using only the radius (at the droplet waist), as seen through an inverted microscope, we simply used the visual cue of the droplets sagging as qualitative confirmation of a tightly packed, minimum tension monolayer. Lastly, we expect the principle of increasing monolayer packing density by decreasing the droplet surface area to be applicable for both lipid-in and lipid-out methods (see Fig. S5, supplementary material). However, as identified in

our previous work,[16] other factors, such as the formation of swollen, inverse micelles in the oil subphase near a partially packed monolayer, can also prevent successful DIB formation when certain lipids are placed in oil.

CONCLUSION

Herein, we demonstrated a simple evaporation-induced monolayer compression technique that enables improved and faster assembly of DIBs, including those comprised of unsaturated lipids such as DOPC and POPC. The technique leverages controlled evaporation to condense the spontaneously self-assembled monolayers, which we found increased the DOPC and POPC bilayer formation success rate from <20% to nearly 100%. It is feasible that this approach could also be used to improve DIB formation from charged lipids such as 1,2-dioleoyl-sn-glycero-3-phosphoglycerol (DOPG). To understand how this method improved bilayer formation, the effects of lateral compression of DOPC and POPC monolayers were studied in comparison to DPhPC using pendant drop tensiometry and Langmuir compression isotherms. Our measurements confirmed that, unlike DPhPC, DOPC and POPC lipids do not spontaneously assemble into maximally packed monolayers. However, controlled evaporation was used to reduce the IFT of DOPC and POPC monolayers to values lower than 1 mN/m, at which point DIB formation became highly repeatable. The approximate reduction in area per lipid induced by 10–60 s of evaporation was found to be c.a. 6% for DOPC and c.a. 16% for POPC lipids. Lastly, the measured electrical properties such as membrane resistance and rupture potential of DIBs formed with DOPC and POPC were found to be in desirable ranges (and comparable to values obtained with DPhPC), thus making them useful platforms for studying transmembrane proteins and ion channels relevant to mammals.

SUPPLEMENTARY MATERIAL

See supplementary material for a tabular summary of prior DOPC DIB studies, material preparations, and experimental details for DIB formation, pendant droplet tensiometry, Langmuir trough experiments, and measuring lipid CMC. Supplementary data are also provided.

ACKNOWLEDGMENTS

The authors acknowledge funding from the Air Force Office of Scientific Research Basic Research Initiative Grant No. FA9550-12-1-0464, and we thank Mr. Subhadeep Koner and Ms. Megan Pitz for their assistance with the POPC DIB experiments. Langmuir Trough compression isotherm measurements were conducted in Dr. Barry Bruce's lab at the Biochemistry, Cellular and Molecular Biology at the University of Tennessee. Pendant drop measurements of interfacial tensions of lipid monolayers were conducted at the Center for Nanophase Materials Sciences, which is a DOE Office of Science User Facility. This manuscript has been authored by UT-Battelle, LLC, under Contract No. DE-AC0500OR22725 with the U.S. Department of Energy. The United States Government retains and the publisher, by accepting the article for publication, acknowledges that the United States Government retains a non-exclusive, paid-up, irrevocable, world-wide license to publish or reproduce the published form of this manuscript, or allow others to do so, for the United States Government purposes.

[1]A. A. Spector and M. A. Yorek, J. Lipid Res. **26**(9), 1015–1035 (1985).
[2]G. Van Meer, D. R. Voelker, and G. W. Feigenson, Nat. Rev. Mol. Cell Biol. **9**(2), 112–124 (2008).
[3]S. Vanni, H. Hirose, H. Barelli, B. Antonny, and R. Gautier, Nat. Commun. **5**, 4916 (2014).
[4]H. Bayley, B. Cronin, A. Heron, M. A. Holden, W. L. Hwang, R. Syeda, J. Thompson, and M. Wallace, Mol. BioSyst. **4**(12), 1191–1208 (2008).
[5]K. Funakoshi, H. Suzuki, and S. Takeuchi, Anal. Chem. **78**(24), 8169–8174 (2006).
[6]W. L. Hwang, M. Chen, B. Cronin, M. A. Holden, and H. Bayley, J. Am. Chem. Soc. **130**(18), 5878–5879 (2008).
[7]P. J. Milianta, M. Muzzio, J. Denver, G. Cawley, and S. Lee, Langmuir **31**(44), 12187–12196 (2015).
[8]M. R. R. de Planque, S. Aghdaei, T. Roose, and H. Morgan, ACS Nano **5**(5), 3599–3606 (2011).
[9]N. Rojko, B. Cronin, J. S. H. Danial, M. A. B. Baker, G. Anderluh, and M. I. Wallace, Biophys. J. **106**(8), 1630–1637 (2014).

[10]G. J. Taylor, F. A. Heberle, J. S. Seinfeld, J. Katsaras, C. P. Collier, and S. A. Sarles, Langmuir **33**(38), 10016–10026 (2017).
[11]J. R. Thompson, A. J. Heron, Y. Santoso, and M. I. Wallace, Nano Lett. **7**(12), 3875–3878 (2007).
[12]G. J. Taylor and S. A. Sarles, Langmuir **31**(1), 325–337 (2015).
[13]N. Tamaddoni, E. C. Freeman, and S. A. Sarles, Smart Mater. Struct. **24**(6), 065014 (2015).
[14]N. Tamaddoni, G. Taylor, T. Hepburn, S. M. Kilbey, and S. A. Sarles, Soft Matter **12**(23), 5096–5109 (2016).
[15]S. Leptihn, O. K. Castell, B. Cronin, E.-H. Lee, L. C. M. Gross, D. P. Marshall, J. R. Thompson, M. Holden, and M. I. Wallace, Nat. Protocols **8**(6), 1048–1057 (2013).
[16]G. A. Venkatesan, J. Lee, A. B. Farimani, M. Heiranian, C. P. Collier, N. R. Aluru, and S. A. Sarles, Langmuir **31**(47), 12883–12893 (2015).
[17]P. Poulin and J. Bibette, Langmuir **14**(22), 6341–6343 (1998).
[18]S. Thutupalli, J.-B. Fleury, A. Steinberger, S. Herminghaus, and R. Seemann, Chem. Commun. **49**(14), 1443–1445 (2013).
[19]N. E. Barlow, G. Bolognesi, S. Haylock, A. J. Flemming, N. J. Brooks, L. M. C. Barter, and O. Ces, Sci. Rep. **7**(1), 17551 (2017).
[20]D.-W. Jeong, H. Jang, S. Q. Choi, and M. C. Choi, Sci. Rep. **6**, 38158 (2016).
[21]S. Nakata, A. Deguchi, Y. Seki, K. Fukuhara, M. Goto, and M. Denda, Thin Solid Films **615**, 215–220 (2016).
[22]H. Kim, K. Kim, H.-R. Lee, H. Jo, D.-w. Jeong, J. Ryu, D.-G. Gweon, and S. Q. Choi, J. Ind. Eng. Chem. **55**, 198–203 (2017).
[23]K. J. Seu, A. P. Pandey, F. Haque, E. A. Proctor, A. E. Ribbe, and J. S. Hovis, Biophys. J. **92**(7), 2445–2450 (2007).
[24]T. Baumgart and A. Offenhäusser, Biophys. J. **83**(3), 1489–1500 (2002).
[25]M. A. Holden, D. Needham, and H. Bayley, J. Am. Chem. Soc. **129**(27), 8650–8655 (2007).
[26]G. A. Venkatesan and S. A. Sarles, Lab Chip **16**(11), 2116–2125 (2016).
[27]G. J. Taylor, G. A. Venkatesan, C. P. Collier, and S. A. Sarles, Soft Matter **11**(38), 7592–7605 (2015).
[28]M. E. Sandison, M. Zagnoni, and H. Morgan, Langmuir **23**(15), 8277–8284 (2007).
[29]P. Mruetusatorn, J. B. Boreyko, G. A. Venkatesan, S. A. Sarles, D. G. Hayes, and C. P. Collier, Soft Matter **10**(15), 2530–2538 (2014).
[30]A. Yasmann and S. Sukharev, Langmuir **31**(1), 350–357 (2015).
[31]M. Ohno, T. Toyota, T. Nomoto, and M. Fujinami, Colloids Surf. A **480**, 85–90 (2015).
[32]K. Y. C. Lee, Annu. Rev. Phys. Chem. **59**(1), 771–791 (2008).
[33]S. Baoukina, L. Monticelli, H. J. Risselada, S. J. Marrink, and D. P. Tieleman, Proc. Natl. Acad. Sci. U.S.A. **105**(31), 10803–10808 (2008).
[34]S. F. Gilmore, A. I. Yao, Z. Tietel, T. Kind, M. T. Facciotti, and A. N. Parikh, Langmuir **29**(25), 7922–7930 (2013).
[35]A. Tsanova, A. Jordanova, and Z. Lalchev, J. Membr. Biol. **249**(3), 229–238 (2016).
[36]Y. Ishitsuka, D. S. Pham, A. J. Waring, R. I. Lehrer, and K. Y. C. Lee, Biochim. Biophys. Acta, Biomembr. **1758**(9), 1450–1460 (2006).
[37]S. Lee, D. H. Kim, and D. Needham, Langmuir **17**(18), 5537–5543 (2001).
[38]D. Needham and D. A. Haydon, Biophys. J. **41**(3), 251–257 (1983).
[39]J. Bigay and B. Antonny, Dev. Cell **23**(5), 886–895 (2012).
[40]T. G. Pomorski, T. Nylander, and M. Cárdenas, Adv. Colloid Interface Sci. **205**, 207–220 (2014).
[41]M. Garten, C. Prévost, C. Cadart, R. Gautier, L. Bousset, R. Melki, P. Bassereau, and S. Vanni, Phys. Chem. Chem. Phys. **17**(24), 15589–15597 (2015).
[42]B. Kollmitzer, P. Heftberger, M. Rappolt, and G. Pabst, Soft Matter **9**(45), 10877–10884 (2013).
[43]M. Jurak, J. Phys. Chem. B **117**(13), 3496–3502 (2013).
[44]K. Nag, J. G. Munro, K. Inchley, S. Schürch, N. O. Petersen, and F. Possmayer, Am. J. Physiol. **277**(6), L1179–L1189 (1999).
[45]F. Giebel, M. Paulus, J. Nase, I. Kiesel, S. Bieder, and M. Tolan, Colloids Surf., A **504**, 126–130 (2016).
[46]V. Fainerman, E. Aksenenko, and R. Miller, Adv. Colloid Interface Sci. **244**, 100–112 (2017).
[47]Q. Lei and C. D. Bain, Phys. Rev. Lett. **92**(17), 176103 (2004).
[48]S. Yefet, E. Sloutskin, L. Tamam, Z. Sapir, M. Deutsch, and B. M. Ocko, Langmuir **30**(27), 8010–8019 (2014).
[49]J. Marqusee and K. A. Dill, J. Chem. Phys. **85**(1), 434–444 (1986).
[50]M. Thoma and H. Möhwald, J. Colloid Interface Sci. **162**(2), 340–349 (1994).
[51]C. Roach, S. E. Feller, J. A. Ward, S. R. Shaikh, M. Zerouga, and W. Stillwell, Biochemistry **43**(20), 6344–6351 (2004).
[52]J. D. Berry, M. J. Neeson, R. R. Dagastine, D. Y. Chan, and R. F. Tabor, J. Colloid Interface Sci. **454**, 226–237 (2015).
[53]P. B. Welzel, I. Weis, and G. Schwarz, Colloids Surf., A **144**(1), 229–234 (1998).